Title:

Spatial and temporal laser pulse shaping for two color excitation

Author(s):

M. B. Hild, M. Safaeisadegh, A. Lindinger

Citation:

"M. B. Hild, M. Safaeisadegh, A. Lindinger, 2022, Optik 250, Part 1, 168293 ; https://doi.org/10.1016/j.ijleo.2021.168293"
Archiviert unter http://dx.doi.org/10.17169/refubium-37644

Spatial and temporal laser pulse shaping for two color excitation

M. B. Hild, M. Safaeisadegh, A. Lindinger*

Institut für Experimentalphysik, Freie Universität Berlin, Arnimallee 14, D-14195 Berlin, Germany

Abstract

Spatial and temporal laser pulse shaping is reported for two adjacent ranges of the laser spectrum. Thereto, two-photon excited fluorescence of dyes is measured for tailored pulses having two different spectral components which possess differently modulated spatial shapes. These particularly designed pulses are formed by using a 4f-temporal liquid crystal pulse shaper followed by a 2D-spatial shaper setup. Increased fluorescence contrasts between different dyes in a cuvette are recorded by selective phase shaping of the two adjacent spectral components. Moreover, two-photon excitation of the two spectral ranges from partially overlapping beams leads to spatially localized fluorescence in the overlap region. This is controlled by utilizing antisymmetric phase functions and can be applied to yield more complex two-photon excited fluorescence structures. The developed temporal and spatial shaping method of two-photon processes has valuable perspectives for optical and biophotonic applications.

Keywords: pulse shaping, optical fibers, polarization, multiphoton excitation
2010 MSC: 00-01, 99-00

1. Introduction

Laser pulse shaping was increasingly investigated in the last years and it was applied in different research fields like coherent control of molecular dynamics

*Corresponding author
Email address: lindin@physik.fu-berlin.de (A. Lindinger*)

[1, 2, 3, 4], biological systems [5], nanooptics [6], and multiphoton transitions by interpulse interference [7, 8]. These interferences were achieved by applying antisymmetric phase functions [9]. The pulse shaping properties were further explored by developing novel pulse shaping schemes for phase and polarization [10, 11] or phase, amplitude, and polarization [12]. Moreover, parametric descriptions of pulse shapes were introduced in order to intentionally control the tailored pulses [13]. Multiphoton microscopy with ultrashort laser pulses [14, 15] is a further relevant topic for the application of pulse shaping, because it allows for selective excitation of different molecules.

By employing spatial pulse shapers it is also feasible to intentionally modulate the spatial profile of a laser beam, particularly in the focal plane of a focussing lens [16, 17]. This is performed by utilizing two dimensional liquid crystal arrays placed in a spatial pulse shaping setup. The theoretical concept of spatial modulation evolves around diffraction and can similarly be applied for continuous laser beams and short laser pulses. Spatially shaped beam profiles were e.g. applied to perform high resolution imaging [18, 19] or microstructuring [20], and first experinments were conducted for limited simultaneous temporal and spatial modulation [21, 22]. Further research in this direction will be of interest to entirely modulate the light field for temporally and spatially controlling photo-induced processes.

Here we report on simultaneous temporal and spatial pulse shaping to intentionally generate complex light fields for efficient two-photon excitation of molecular probes. Scans of antisymmetric phase functions for spatially separated light components with adjacent spectral ranges will be conducted in order to receive an increased two-photon excited fluorescence contrast. Particularly, we will demonstrate excitation by two adjacent spectral ranges from partially overlapping beams which results in localized two-photon excited fluorescence spots in the overlap region. The fluorescence yield will be influenced by antisymmetric phase functions and more detailed two-photon excited fluorescence structures will be demonstrated. The presented pulse shaping approach will give rise to novel biophotonic techniques.

2. Experimental setup

The schematic experimental setup is presented in Fig. 1. A frequancy-doubled Nd:YVO_4 laser (Verdi V, Coherent, Inc.) pumps a broadband titanium sapphire laser oscillator (Femtosource Compact, Femtolasers) having an average power of 300 mW, a repetition rate of 75 MHz, a center wavelength at 805 nm, and a bandwidth of about 80 nm. The emitted laser beam is guided through a 4f-pulse shaper with a computer controlled liquid crystal light modulator (SLM 640, Cambridge Research Instruments) with two adjacent liquid crystal arrays having optical axes at $\pm 45°$ to the horizontal. This enables the independent modification of phase and polarization.

The outcoming temporally shaped laser pulses are guided on a 2D-array of a spatial light modulator (PLUTO-NIR-015-C, HOLOEYE Photonics AG) in order to generate differing spatial shapes of the polarization components. The 2D-array moduator has a rectangular shape (15.36 mm x 8.64 mm) with 1920 x 1080 liquid crystal elements, and an attached mirror to reflect the beam back through the liquid crystals. The spatial modulator is programmed to inscribe the phase function on 1000 x 1000 pixels. The light exposed range of the beam profile is adjusted to be in this quadratic active region to form a spatially modulated laser profile.

The tailored laser beam is then focussed by a 2f-setup with a lens (f = 300 mm) located 300 mm behind the 2D-modulator into a quartz cuvette in order to generate spatially shaped light spots in the focal plane. This design is favorable since it provides the condition to employ the spatial 2D-Fourier transformation. Furthermore, a polarizer at 45° to the horizontal is placed in the light path after the spatial shaper to create a linear polarization with equal horizontal and vertical polarization components. The cuvette is filled with the dyes rhodamine B ($rhoB$) or coumarin 47 ($cou47$) dispersed in glycerol. These dyes were chosen for the two-photon excitations because they have high quantum yields [23, 24].

The outcoming fluorescence passes an IR glass filter (BG 39), where the laser stray light is reduced, and it is finally focussed on a camera (AW335, Ausdom

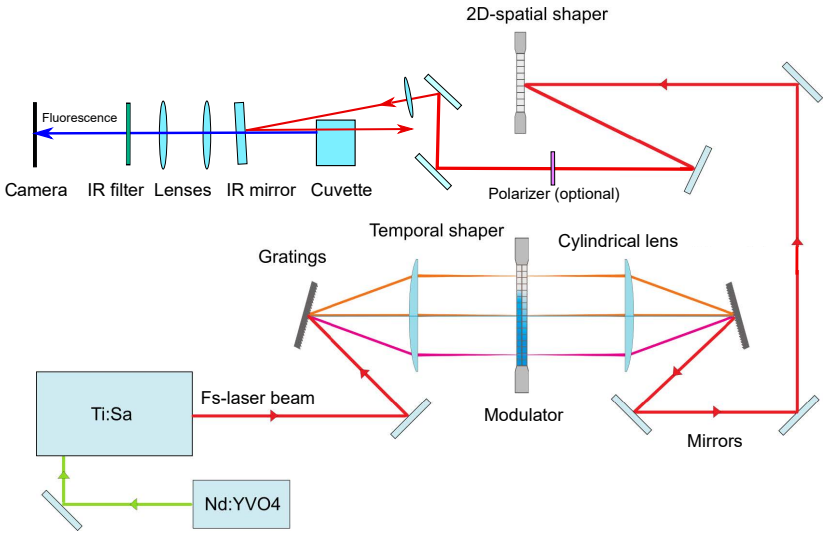

Figure 1: Schematic experimental setup comprising a fs-laser (Ti:Sa), a temporal pulse shaper, a subsequent spatial 2D-shaper, a cuvette, and a fluorescence detection stage. A light polarizer can be inserted after the spatial modulator.

Inc.). The measurements are conducted for top view detection of the two-photon excited fluorescence with the detector facing the surface of the cuvette. Thereto, a dielectric reflecting mirror for wavelengths around 800 nm is installed in order to guide the laser beam on the glass surface of the cuvette, whereby the fluorescence light transmits the mirror (see Fig. 1). The described top view setup enables concomitant excitation and detection on the surface normal. An optimization algorithm by phase resolved interferometric spectral modulation (PRISM) [26] is performed before starting the experiments in order to obtain the phase retardances required for shortest pulses. Thereto a diode, which gives a signal for two-photon excitation, is placed close to the interaction region and its maximal yield is searched by the algorithm.

For PRISM the liquid crystal elements of the temporal shaper (pixels) are randomly assigned to groups. Only the pixels of one group are changed at a time and all other pixels are kept stationary in order to give a stable reference. The following steps are then performed for one group after the other. For frequency

allocation the interval from $\pi/2$ to π is uniformly divided into n scalars, where n is the number of pixels in a group. Every scalar is allocated to one pixel in the group.

In the measurement procedure, for every step the phase of every pixel is shifted by its allocated scalar, respectively. For every step, the nonlinear intensity is measured using a two photon diode. That results in one scalar per step. 4n steps are performed. The intensity values are plotted against the number of the respective step. The nonlinear signal shows a beating pattern.

A Fourier transform is performed for the intensity against number of the respective step. The Fourier transform gives a term at each frequency, that was allocated in the frequency allocation. Every frequency will have an associated phase. For every pixel in the group, the associated phase is subtracted to the phase of the pixel.

The algorithm does not give a transform-limited pulse after one round in general, since the reference field is not transform-limited. However, the pulse shape converges into a transform-limited pulse [26]. The number of iterations depends on the quality of the starting phase function. This leads to a flat spectral phase which is a prerequisite for phase-controlled measurements, and e. g. allows for precise generation of third order phases.

3. Results

3.1. Contrast improvement between dyes by two color excitations

For imaging applications it is important to have a high contrast between different substances. This is the motivation for the use of simultaneous temporally and spatially shaped pulses to perform selective two-photon excitations of different dyes. Antisymmetric phase functions for spatially separated light components with adjacent spectral ranges are utilized to achieve an enhanced two-photon excited fluorescence contrast. Thereto, the liquid crystals of the modulator from the temporal shaper are adjusted to turn the polarization of

one spectral range by 90°, hence in the vertical direction. The resulting two perpendicular polarization components are then directed on the spatial modulator where the horizontal polarization component is modulated. This leads to two spatially separated spots in the focal plane whereby the horizontal polarization component is vertically upshifted by applying a linear spatial phase using the Zernike polynominal Z_1^{-1} with appropriate prefactors inscribed on the 2D-array, whereas the vertical polarization component is not shifted. Furthermore, phase functions $\phi(\omega) = \frac{b_3}{6}(\omega - \omega_0)^3$ with a third order phase factor $b_3 = 1 \cdot 10^4$ fs^3 and differently tuned phase center frequencies ω_0 are written on the temporal pulse shaper, simultaneously acting on both polarization components. These phase center frequencies lead to spectrally narrow two-photon maxima due to constructive interference close to ω_0 as described in [9] which allows for selective excitation.

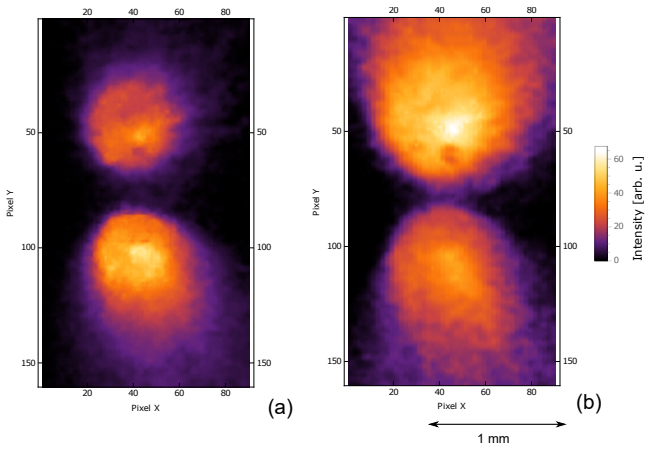

Figure 2: Fluorescence spots of spatially and temporally shaped pulses for the spectrally dividing cut wavelength at 820 nm for rhodamine B (a) and coumarin 47 (b), respectively. The differing intensities demonstrate selective two-photon excitation.

Fig. 2 shows two fluorescence spots for the phase center wavelength $\lambda_0 = 2\pi c/\omega_0$ at the spectrally dividing cut wavelength of 820 nm for rhodamine B (a) and coumarin 47 (b), respectively. The spots exhibit differing intensities for the two dyes, with a more intense upper spot for rhodamine B and a more

intense lower spot for coumarin 47. This indicates that a selective two-photon excitation of the different dyes can be performed with such modulated pulses.

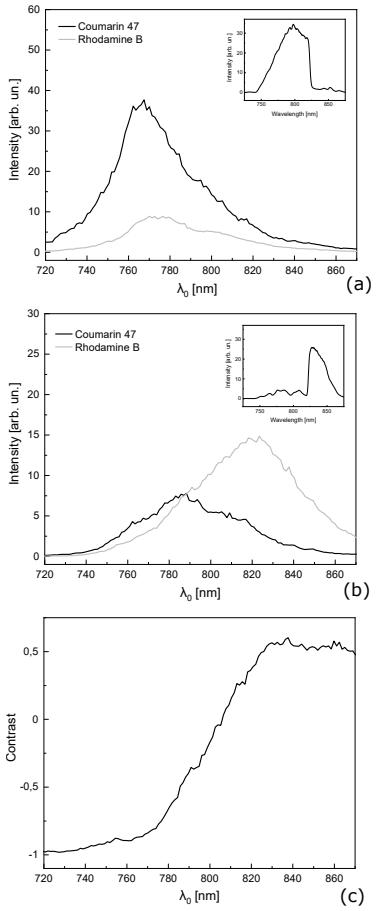

Figure 3: Scans of the phase center wavelength for the third order phase functions at the upper fluorescence spot (a) and at the lower spot (b). The insets display the corresponding laser spectra. The contrast of the two fluorescence spots between rhodamine B from the lower graph and coumarin 47 from the upper graph is displayed in (c).

Scans of the phase center wavelength λ_0 for the third order phase functions are performed for the two dyes at the upper fluorescence spot (Fig. 3(a)) and at the lower spot (Fig. 3(b)). The scans show phase center wavelength dependent fluorescence intensities due to the features of these particular third order

phase functions [9]. The laser spectra of the exciting perpendicular polarization components were each recorded by a fiber spectrometer (Ocean Optics, Inc.). The vertical component was generated by turning the polarization of a part of the spectrum which is then missing in the other component.

Fig. 3(c) presents the contrast $c = (I_{rhoB,low} - I_{cou47,up})/(I_{rhoB,low} + I_{cou47,up})$ of the two fluorescence spots, where I_{up} and I_{low} indicate the intensities of the upper and lower spots, respectively. This shows the phase-tailored major excitation of a specific dye by one spectral component and a simultaneous excitation of another dye by the other spectral component, which leads to a large contast difference of about 1.8 between the dyes. This demonstrates the high selectivity of this pulse shaping method.

3.2. Spatial fluorescence by two color excitation

Two-photon transitions provide the opportunity to utilize two different frequency ranges for excitation. Partial overlap of the two light fields will allow for a localized two-photon excitation which can be observed by the induced fluorescence signal. Here we realize this with two adjacent ranges in the laser pulse spectrum. The fluorescence yield will be influenced by antisymmetric phase functions which enable constructive two-photon excited fluorescence close to the antisymmetry point of the phase function.

In a preliminary experiment scans of the phase antisymmetry point of the third order phase functions were performed for the added two fluorescence spots of coumarin 47 with a third order phase factor of $b_3 = 1 \cdot 10^4$ fs^3 and for the fluorescence of the entirely overlapped spots (see Fig. 4). The cut wavelength between the two frequency ranges is at 810 nm where the two spots have almost equal intensity. The black line shows the signal for two separate spots while the grey line displays the fluorescence for totally overlapping spots. For two separate spots one observes two maxima, whereas for the overlapping spots a higher broad single maximum is obtained at a wavelength between the two maxima. This indicates the occurrence of constructive interference between the two parts of the laser spectrum due to antisymmetric phase functions in the

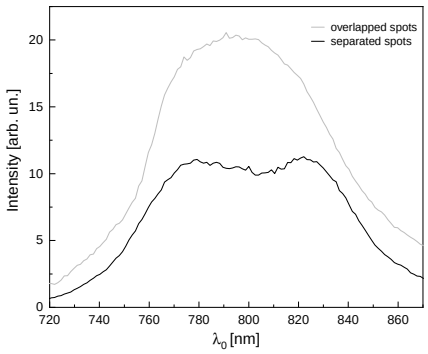

Figure 4: Scans of the phase center wavelength λ_0 of the third order phase functions are presented for the sum of the two fluorescence spots of coumarin 47 (black line) and the fluorescence of the entirely overlapped spots (gray line).

overlapping case.

In order to investigate the spatial combination of the two spots they are partially overlapped and the induced fluorescence is recorded by a camera. The images for three values of λ_0 are taken (see Fig. 5), where the first optimizes the lower spot (a), the second the overlap region (b), and the third the upper spot (c). The added intensities for vertical direction are presented in Fig. 5(d). In the first case the phase center wavelength was chosen at 840 nm to selectively excite with the lower light component and in the last case at 760 nm to excite with the upper light component. The overlapped case is received with a phase center wavelength close to the cut wavelength between the two spectral components at 810 nm. Here, the two spectral ranges both contribute to the induced fluorescence signal which leads to a new maximum localized between the upper and lower spot. Hence, a spatially localized fluorescence by two-photon excitation is obtained.

With the spatial pulse shaper it is possible to produce more complex fluorescence structures. Constructive interference between these structures and other light components will generate novel fluorescence intensity shapes. This

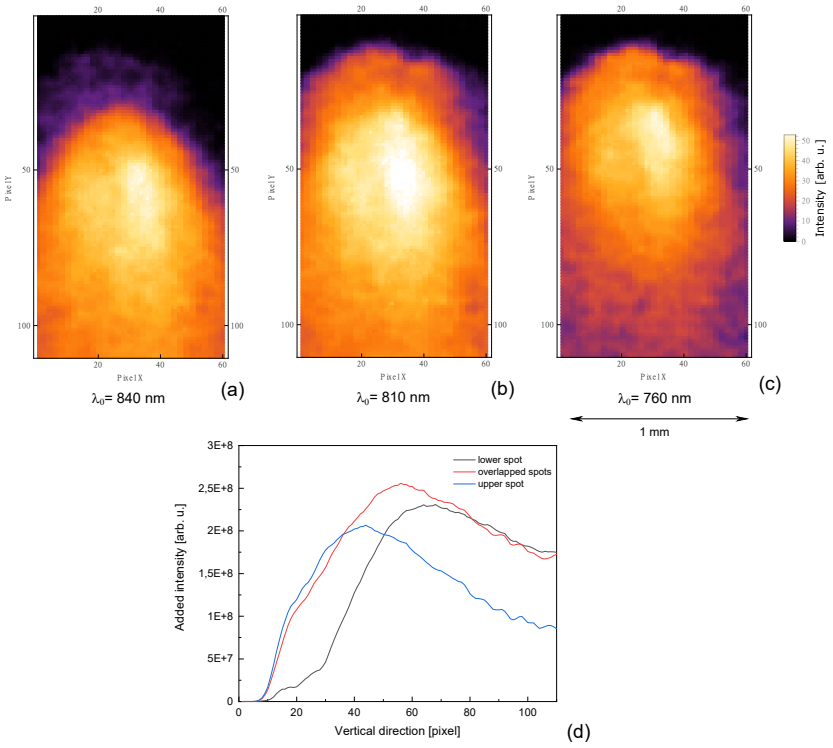

Figure 5: Fluorescence images for three phase center values with the selective excitation of the lower fluorescence spot (a), the excitation of the overlap region (b), the excitation of the upper spot (c), and the added intensities for vertical direction (d). The overlapped case is achieved with λ_0 close to the cut wavelength between the two spectral components, where both spectral ranges contribute to the induced fluorescence signal.

is demonstrated in Fig. 6 where a two spot component is produced by writing a one-dimensional rectangular phase grating on the 2D-modulator with an amplitude of 1.8 and a period of 80 pixels. The generated two spot component is partially overlapped with a single spot component. The images display the selective excitation at 840 nm for the single spot light field, the overlapped structure, and the selective excitation at 760 nm for the two spots.

The overlapped profile is achieved with λ_0 close to the cut wavelength at 810 nm between the two spectral components. The overlapped case has a new structure due to the combination of the two spot and the single spot light fields

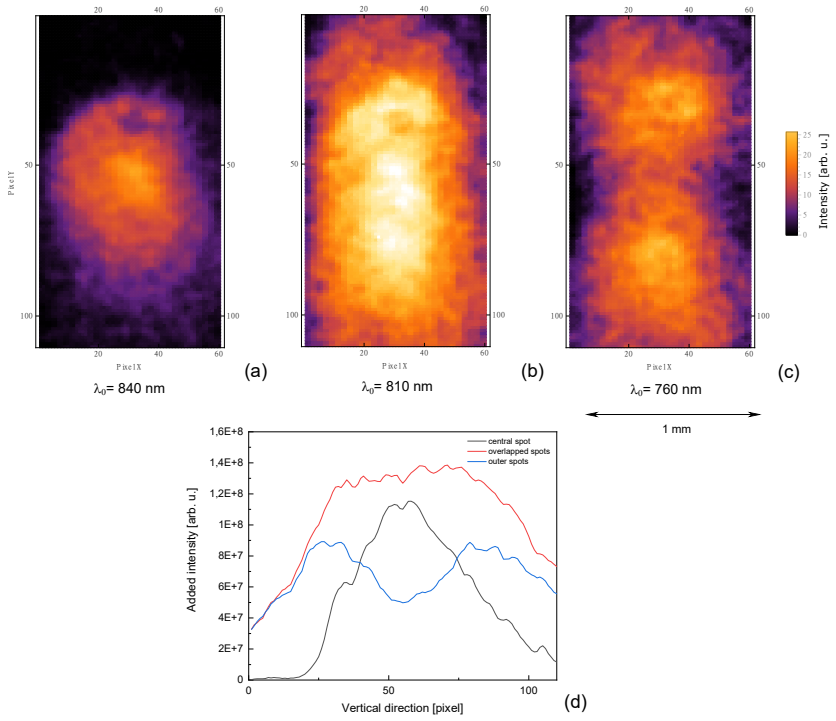

Figure 6: Fluorescence images for three phase center values with the selective excitation of the single fluorescence spot (a), the excitation of the overlap region (b), the excitation of the two spots (c), and the added intensities for vertical direction (d). The overlapped case shows a novel structure with high intensity between the single and double fluorescence spots.

with indications for high intensities between the single and double spots. It should be noted that it is feasible to strongly modify the spatial profiles by spectral phase modulation. This combined spatial and temporal modulation method allows for versatile pulse shaping.

4. Conclusions

We performed spatial and temporal pulse shaping for two adjacent ranges of the laser spectrum for two-photon excited fluorescence. The laser pulses having two different spatial components were generated by a temporal pulse shaper and a subsequent spatial shaper via polarization modulation. We obtained en-

hanced fluorescence contrasts between different dyes by selective phase shaping of the two adjacent spectral components. Furthermore, partial overlap of the two beams with different spectral ranges resulted in localized spatial two-photon excited fluorescence spots in the overlap region. Antisymmetric phase functions were employed to modify the two-photon excitation processes which enables various fluorescence structures. The presented temporal and spatial shaping approach for two-photon transitions will lead to prospective biophotonic methods.

Acknowledgements

We thank Prof. W. Kuch and I. Kumberg for support. The Helmut Fischer Foundation is acknowledged for financial aid.

References

[1] T. Brixner and G. Gerber, Quantum control of gas-phase and liquid-phase femtochemistry, ChemPhysChem **4** (2003) 418-438.

[2] G. Vogt, G. Krampert, P. Niklaus, P. Nuernberger, G. Gerber, Optimal control of photoisomerization, Phys. Rev. Lett. **94** (2005) 068305.

[3] A. Assion, T. Baumert, M. Bergt, T. Brixner, B. Kiefer, V. Seyfried, M. Strehle, G. Gerber, Control of chemical reactions by feedback-optimized phase-shaped femtosecond laser pulses, Science **282** (1998) 919-922.

[4] A. Lindinger, C. Lupulescu, M. Plewicki, F. Vetter, S. M. Weber, A. Merli, and L. Wöste, Isotope selective ionization by optimal control using shaped femtosecond laser pulses, Phys. Rev. Lett. **93** (2004) 033001.

[5] W. Wohlleben, T. Buckup, J. L. Herek, M. Motzkus, Coherent control for spectroscopy and manipulation of biological dynamics, ChemPhysChem **6** (2005) 850-857.

[6] M. Aeschlimann, M. Bauer, D. Bayer, T. Brixner, F. J. Garcia de Abajo, W. Pfeiffer, M. Rohmer, C. Spindler, F. Steeb, Adaptive subwavelength control of nano-optical fields, Nature **446** (2007) 301-304.

[7] K. A. Walowicz, I. Pastirk, V. V. Lozovoy, M. Dantus, Multiphoton intrapulse interference. 1. Control of multiphoton processes in condensed phases, Phys. Chem. A **106** (2002) 9369-9373.

[8] V. V. Lozovoy and M. Dantus, Systematic control of nonlinear optical processes using optimally shaped femtosecond pulses, ChemPhysChem **6** (2005) 1970-2000.

[9] V. V. Lozovoy, I. Pastirk, K. A. Walowicz, and M. Dantus, Multiphoton intrapulse interference. 2. Control of two- and three-photon laser induced fluorescence with shaped pulses, J. Chem. Phys. **118** (2002) 3187-3196.

[10] T. Brixner and G. Gerber, Femtosecond polarization pulse shaping, Opt. Lett. **26** (2001) 557-559.

[11] L. Polachek, D. Oron, and Y. Silberberg, Full control of the spectral polarization of ultrashort pulses, Opt. Lett. **31** (2006) 631-633.

[12] F. Weise, A. Lindinger, Full control over the electric field using four liquid crystal arrays, Opt. Lett. **34** (2009) 1258-1260.

[13] F. Weise and A. Lindinger, Full parametric pulse shaping in phase, amplitude, and polarization using an effective four array modulator, Appl. Phys. B **101** (2010) 79-91.

[14] W. Denk, J. H. Strickler and W. W. Webb, Two-photon laser scanning fluorescence microscopy, Science **248** (1990) 73-76.

[15] S. Perry, R. Burke, and E. Brown, Two-Photon and Second Harmonic Microscopy in Clinical and Translational Cancer Research, Ann. Biomed. Eng. **40** (2012) 277.

[16] N. Sanner, N. Huot, E. Audouard, C. Larat, J.-P. Huignard, Programmable focal spot shaping of amplified femtosecond laser pulses, Opt. Lett. **30** (2005) 1479-1481.

[17] C. Maurer, A. Jesacher, S. Bernet, M. Ritsch-Marte, What spatial light modulators can do for optical microscopy, Laser Photonics Rev. **5** (2011) 81-101.

[18] S. Hell, J. Wichmann, Breaking the diffraction resolution limit by stimulated emission: stimulated-emission-depletion fluorescence microscopy, Opt. Lett. **19** (1994) 780-782.

[19] G. Moneron, S. Hell, Two-photon excitation STED microscopy, Opt. Exp. **17** (2009) 14567-14573.

[20] N. Sanner, N. Huot, E. Audouard, C. Larat, J.-P. Huignard, Direct ultrafast laser micro-structuring of materials using programmable beam shaping, Opt. Lasers Eng. **45** (2007) 737-741.

[21] T. Feurer, J. C. Vaughan, R. M. Koehl, K. A. Nelson, Multidimensional control of femtosecond pulses by use of a programmable liquid-crystal matrix, Opt. Lett. **27** (2002) 652-654.

[22] H. Suchowski, A. Natan, B. D. Bruner, Y. Silberberg, Spatio-temporal coherent control of atomic systems: weak to strong field transition and breaking of symmetry in 2D maps, J. Phys. B **41** (2008) 074008.

[23] M. J. Snare, F. E. Treloar, K. P. Ghiggini, P. J. Thistlethwaite, The photophysics of rhodamine B, J. Photochem. **18** (1982) 335-346.

[24] R. F. Kubin, A. N. Fletcher, Fluorescence quantum yields of some rhodamine dyes, J. Luminescence **27** (1982) 455-462.

[25] J. H. Richardson, L. L. Steinmetz, S. B. Deutscher, W. A. Bookless, W. L. Schmelzinger, Measurement of fluorescence lifetimes of coumarin laser dyes with a mode-locked krypton ion laser, Z. Naturforsch. **33a** (1978) 1592–1593.

[26] T. Wu, J. Tang, B. Hajj, and M. Cui, Phase resolved interferometric spectral modulation (PRISM) for ultrafast pulse measurement and compression, Opt. Express **19** (2011) 12961-12968.

[27] N. A. Carvajal, C. H. Acevedo, Y. T. Moreno, Generation of perfect optical vortices by using a transmission liquid crystal spatial light modulator, Int. J. Opt. **2017** (2017) 6852019.

[28] A. Patas, G. Achazi, N. Hermes, M. Pawłowska, A. Lindinger, Influence of nonlinear effects on the three-photon excitation of L-tryptophan in water using phase-shaped pulses, Applied Physics B: Lasers and Optics **112** (2013) 579-586.

[29] G. M. van Dam and G. Themelis, L. M. A. Crane, N. J. Harlaar, R. G Pleijhuis, W. Kelder, A. Sarantopoulos, J. S. de Jong, H. J. G. Arts, A. G. J. van der Zee, J. Bart, P. S. Low, V. Ntziachristos, Intraoperative tumor-specific fluorescence imaging in ovarian cancer by folate receptor- a targeting: first in-human results, Nat. Med. **17** (2011) 1315-1319.

[30] Y. Urano, D. Asanuma, Y. Hama, Y. Koyama, T. Barrett, M. Kamiya, T. Nagano, T. Watanabe, A. Hasegawa, P. L. Choyke, H. Kobayashi, Selective molecular imaging of viable cancer cells with pH-activatable fluorescence probes, Nat. Med. **15** (2009) 104-109.